INTERNATIONAL JOURNAL OF COMMUNICATION SYSTEMS
Int. J. Commun. Syst. (2015)
Published online in Wiley Online Library (wileyonlinelibrary.com). DOI: 10.1002/dac.3086

Integrated power saving for relay node and user equipment in LTE-A

Chun-Chuan Yang[1], Jeng-Yueng Chen[2,*,†], Yi-Ting Mai[3] and Hsieh-Hua Liu[1]

[1]*Dept. of Computer Science and Information Engineering, National Chi Nan University, Puli, Nantou County, Taiwan*
[2]*Dept. of Information Networking Technology, Hsiuping University of Science and Technology, Taichung City, Taiwan*
[3]*Dept. of Sport Management, National Taiwan University of Sport, Taichung City, Taiwan*

SUMMARY

By introduction of relay nodes, LTE-Advanced can provide enhanced coverage and capacity at cell edges and hot-spot areas. The authors have been researching the issue of power saving in mobile communications technology such as WiMax and Long Term Evolution (LTE) for some years. Based on the previous idea of load-based power saving, two strategies each with associated schemes to integrated relay nodes and user equipment in power saving are proposed in the paper. Simulation study shows the benefit of the proposed schemes in terms of better power saving than the standard-based scheme at the cost of moderately increased delay. Extended discussion about the impact of different load distribution among user equipments and the impact of a worse backhaul link on power saving is also presented in the paper. Copyright © 2015 John Wiley & Sons, Ltd.

Received 29 April 2015; Revised 15 August 2015; Accepted 11 October 2015

KEY WORDS: LTE-A; power saving; LBPS; relay node

1. INTRODUCTION

Nowadays, wireless communications plays an integral role in our daily life from weekdays to weekends. As wireless communications becomes increasingly available on newer and faster mobile devices, people's interactions with their society, culture and even one another start to change. The fourth generation (4G) of wireless standards has been specified by the International Telecommunications Union) to meet the peak speed requirement of 100 Mbps for a mobile connection and 1 Gbps for stationary connections. The 4G service is set to offer a fast and secure all-IP, roaming mobile broadband solution to devices such as 4G smartphones that require internet access with speed intensive network applications, including on-demand High Definition Television (HDTV), IP telephony, on-demand gaming, and high-speed internet access.

As a candidate 4G system, *LTE-Advanced* (*LTE-A*) has become the fastest developing mobile communication technology in recent years. Compared with its previous version of *Release 8* [1], LTE-A (*Release 10* and up) aims to provide higher capacity and speed with some enhanced features, including the introduction of the *relay nodes* (*RNs*). RN architecture [2] was initially studied in *Release 9*, and the specification of fixed RN was first included in *Release 10* [3] in order to extend the coverage of high data rates and improve the cell-edge throughput. Currently, 3GPP is moving towards mobility support for RN [4]. With the help of RN, the radio link between *eNB* (the base station) and the user equipment (*UE*) has become two hops as displayed in Figure 1. The link

*Correspondence to: Jeng-Yueng Chen, Dept. of Information Networking Technology, Hsiuping University of Science and Technology, Taichung City, Taiwan.
†E-mail: jychen@ieee.org

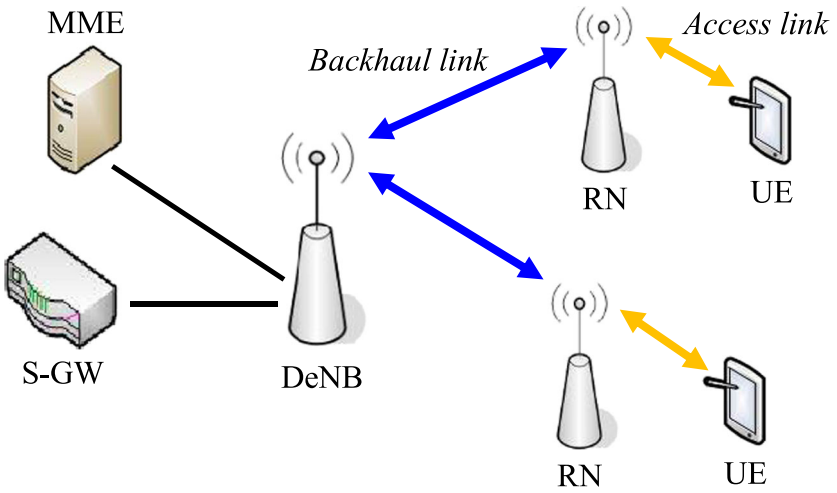

Figure 1. Using relay nodes in LTE-A.

between eNB (also called the *donor eNB* or *DeNB*) and RN is referred to as *the backhaul link*, while the link between RN and UE is referred to as *the access link*. With respect to the usage of spectrum, RN's operation can be divided into *inband* and *outband* types. An RN is said to be inband if the backhaul link and the access link are on the same carrier frequency, and outband if not.

In addition to the improvement of channel capacity and radio coverage, energy saving also plays an important role in modern mobile communications. *Discontinuous reception mode* (*DRX*) is supported in LTE/LTE-A in order to conserve UE's power. One DRX cycle consists of an '*Opportunity for DRX period*' (radio off) during which the UE can skip reception of downlink channels and an '*ON duration*' (radio on) during which the UE should monitor the physical downlink control channel (PDCCH) to identify downlink data. The *inactivity timer* is used to trigger the start of a DRX cycle in the *RRC_connected* state. The parameterization of the DRX cycle involves a trade-off between battery saving and access latency, which is also the main focus of some related work [5–7].

The authors have been researching power-saving mechanisms for some years. The idea of *load-based power saving* (*LBPS*) and associated schemes were proposed for IEEE 802.16 [8, 9]. Extension work of LBPS for UE power saving in LTE was also proposed [10]. In this paper, revised LBPS schemes integrating RN and UE power saving in LTE-A are proposed. Note that the type of RN focused in the paper is *Type 1 RN*, which provides half duplex inband transmissions and controls its cell with its own identity as if it is a Release 8 eNB. Simulation study has demonstrated that with the proposed schemes, a good level of power saving at both RN and UE can be effectively achieved. The remainder of the paper is organized as follows. In Section 2, a survey of RN related research work and our previous work of LBPS are presented. Proposed integrated LBPS schemes for LTE-A are presented in Section 3. Performance evaluation is presented in Section 4. Finally, Section 5 concludes this paper.

2. RELATED WORK

2.1. Relay node related research

Most of the RN related work focused on resource allocation of the backhaul link for Type 1 RN. By considering the idea that scheduling on the backhaul link should guarantee the amount of data relayed to the RN well matching with the data required on the access link for each relayed UE, the authors in [11] proposed a request-and-send mechanism for adjusting UE priority on the backhaul link. A data-request signal is triggered by the RN if the queue length of a UE at RN is below a specific threshold, which is according to the estimated throughput achievable on the access link. In [12], the authors formulated a weighted power minimization problem for bandwidth sharing of the backhaul link and the access link under constraints on required rate, bandwidth, and transmit power.

DOI: 10.1002/dac

It is concluded that adaptive bandwidth sharing provides better power gain as compared witb fixed allocation of bandwidth per link. The authors in [13] identified the issue that performing a multi-hop transmission requires more radio resources than a single-hop transmission and analyzed how the available resource should be allocated to the RN in order to maximize throughput and fairness. The authors concluded that if the backhaul link is more efficient than the eNB access link (eNB-UE), cell throughput and relay throughput can both be maximized by choosing a relay throughput maximal solution. However, if the eNB access link instead is more efficient, the cell throughput will be maximized by not using the RNs at all.

A resource allocation algorithm that aims to maximize the throughput of worst UEs in relay enhanced networks was proposed in [14] to calculate the resource allocation among DeNB-RN transmission, RN-UE transmissions, as well as DeNB-UE transmissions in backhaul subframes and access subframes. In [15], a two-step backhaul resource allocation scheme based on relay buffer level was proposed. In the first step, the transmission demand for an RN is calculated according to the residual buffer space at the RN as well as the data amount queueing at DeNB. In the second step, DeNB allocates resources to RNs to minimize the used resource blocks in the subframe. Uplink resource allocation for RN was addressed in [16], in which a co-scheduling mechanism at DeNB for cellular UEs and RNs during the backhaul subframes was proposed. In [17], the benefits of relaying was investigated by comparing the transmission rate of both direct transmission and relaying. It is shown that relaying achieves signal-to-noise power ratio gain over direct transmission because of less path loss, but with several relaying penalties, including a lower multiplexing gain (due to half-duplex), a lower transmit power, and a higher outage requirement at each hop (due to multi-hop).

In addition to resource allocation, buffering behavior at RN also plays an important role in performance. Considering the mismatch of the link quality between the backhaul link and access links, the authors in [18] analyzed the impact of the buffer size at RN on buffer overflows (leading to packet loss) and underflows (leading to waste of resource) and concluded that the size of the buffer at RN can positively influence the throughput performance. In [19], the authors proposed an analytical model for buffer overflow and underflow problems and designed a dynamic flow control algorithm to minimize the probabilities of buffer overflow and underflow.

Selection of DeNB for an RN was addressed in [20], in which the main parameters considered for selection optimization include the network load, the inter-DeNB handover, and the reconfiguration overhead. On the other hand, RN selection for UEs was also addressed in some research works. In [21], aiming for maximizing the total throughput in the uplink, an optimal joint RN selection, sub-carrier assignment and power allocation scheme under total power constraint was proposed. In [22], the authors considered energy efficiency and sleep operation of RN in RN selection and constructed an analytical model for RN's DRX operation, in which an energy-efficient RN selection scheme was proposed. Mechanisms of multiplexing data from different UE bearers over the backhaul link were studied in [23]. Instead of reusing LTE Release 8 logical channel IDs to separate the bearers of different users or by using the 16-bit UE ID in a multiplexing header, the authors proposed a dynamic multiplexing scheme, in which the proposed variable-length multiplexing header depends on the number of relayed UEs and the number of active bearers. The authors in [24] addressed the network architecture aspects for RN mobility by taking into account the additional requirements such as the group mobility and persistent IP connectivity during handover and identified the more appropriate architecture alternative. By considering that the UEs may suffer from worse channel conditions if handovers between the RNs and eNB are not correctly and immediately determined by the eNB, the authors in [25] proposed a prediction-based scheme to allow eNBs to make potential handover decisions within the UE's reporting period for channel quality. In the proposed scheme, the channel qualities are predicted based on the partially observable Markov decision process using the past information, and handover decision can be made without completely exact measurement reports from UEs.

2.2. Previous work of load-based power saving

The basic idea of LBPS is to take advantage of traffic modeling in determining the length of the sleep period. The traffic in LBPS is assumed to be a *Poisson* process in order to take advantage of

DOI: 10.1002/dac

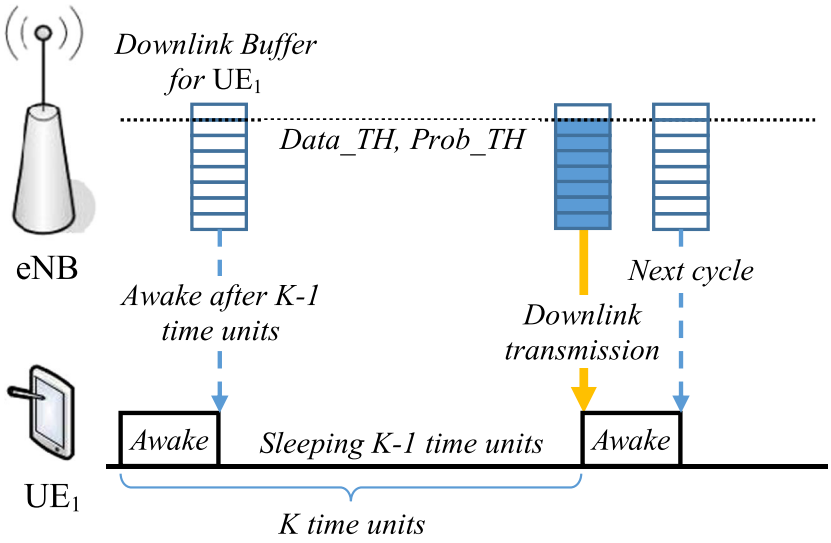

Figure 2. Load-based power saving.

the multiplexing property. Taking a single user node (e.g., a single UE in LTE) with its downlink traffic as an example, the base station estimates the traffic load and calculates the length of the sleep period in order for the accumulated data in the base station's buffer reaching a predefined level as illustrated in Figure 2. The predefined level consists of two threshold parameters: *Data_TH* and *Prob_TH* as shown in Figure 2. The length of the sleep period is calculated by making the amount of accumulated data exceeding *Data_TH* with probability higher than *Prob_TH*.

As displayed in Figure 2, an awake-and-sleep cycle in LBPS is composed of the current awake period and the following sleep period. A basic function, namely $P_{Acc}(K, Data\_TH)$, was defined in the authors' previous work to calculate the probability of data accumulation exceeding *Data_TH* over K time units in a row. The length of the next awake-and-sleep cycle, denoted by K^*, is calculated by another function, namely *LengthAwkSlpCyl* (λ, *Data_TH*), where λ is the estimated input load. The calculation of the two function is as follows:

$$P_{Acc}(K, Data\_TH) = \sum_{i=Data\_TH+1}^{\infty} \frac{e^{-\lambda KT}(\lambda KT)^i}{i!} = 1 - \sum_{i=0}^{Data\_TH} \frac{e^{-\lambda KT}(\lambda KT)^i}{i!}$$

$$K^* = LengthAwkSlpCyl(\lambda, Data\_TH) = Min\{K | P_{Acc}(KData\_TH) \geq Prob\_TH\}$$

The value of *Data_TH* could be any value theoretically, but in practice, it is suggested to set its value as the amount of data that can be served within the basic time unit of transmission scheduling (e.g., a *transmission time interval* or *subframe* in LTE) in order to obtain a good balance between power saving and delay performance. In LTE, the amount of data that can be served in a subframe is fluctuated and affected by the link quality. Therefore, applying LBPS in LTE requires estimation of the capacity in a subframe. In the authors' previous work [10], *channel quality indicator* (*CQI*) were used in estimating subframe capacity, and two types of CQI reporting, namely, *wideband reporting* and *full-sub-band reporting* were addressed.

For the general case of multiple users in the network, three LBPS schemes, namely, *LBPS-Aggr*, *LBPS-Split*, and *LBPS-Merge* were proposed to deal with multiplexing users in sleep scheduling. *LBPS-Aggr* is the simplest scheme that treats all traffic as an aggregate flow in determining the length of the sleep period and synchronizes all UEs in sleep scheduling as illustrated in the upper part of Figure 3. The idea of *LBPS-Split* is motivated by the following observation on the sleep pattern of *LBPS-Aggr*. If we place the awake subframe of some UEs in a different part of a cycle, the cycle length could be extended because the load of each split group is less than the total load

DOI: 10.1002/dac

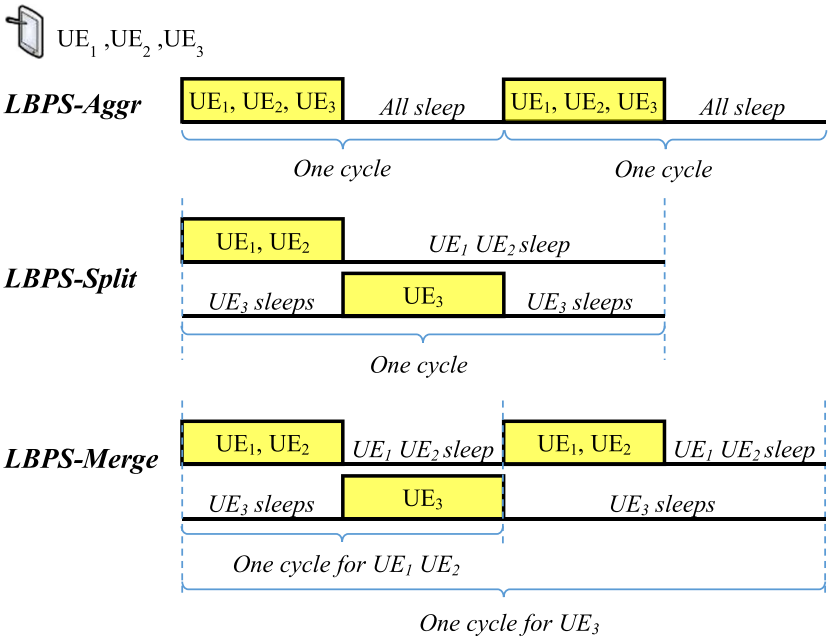

Figure 3. Load-based power saving schemes.

used in *LBPS-Aggr*. As illustrated in the middle part of Figure 3, a larger cycle is made by splitting UEs into two groups ($UE_1 + UE_2$ and UE_3), resulting in better power-saving performance.

LBPS-Merge is motivated by the idea that given a predefined level for data accumulation, the best case for a UE in terms of power saving is to make the UE a single-member group, which results in the largest sleep period for the UE. Because a different group in general has a different cycle length, in order to efficiently find a feasible sleep schedule for all groups, the cycle length for each group in *LBPS-Merge* is converted to the closest and smaller power of 2. In the case that a feasible sleep schedule cannot be found for the current state of grouping, iterated merging operation of some groups is performed until a feasible sleep schedule is found. As illustrated in the lower part of Figure 3, there are two groups in the sleep schedule: the group of UE_1+UE_2 with two-subframe cycle and the group of UE_3 with four-subframe cycle.

3. INTEGRATED POWER-SAVING SCHEMES

3.1. Integration strategies

With the presence of RN for the radio link, downlink transmission first goes through the backhaul link and then the access link. That is, before RN can serve UEs in a subframe, it must first receive data from DeNB in a previous subframe. Therefore, the awake subframe for receiving data on the backhaul link must be taken into consideration in designing sleep scheduling for RN. Furthermore, as mentioned in Section 1, we focus on Type 1 RN, and a Type 1 RN is in charge of transmission scheduling for its underlying UEs, which makes RN the better position than DeNB to perform LBPS schemes and issue DRX commands to UEs. We also assume that the quality and capacity of the backhaul link are much better than the access link as in the case of fixed RN to simplify the design of the LBPS schemes. The impact of low-quality backhaul link on power saving performance is investigated in Section 4.

There are naturally two strategies to integrate RN and UEs in sleep scheduling: *UE-first* and *RN-first*. In the UE-first strategy, power saving for UEs is the first concern, and LBPS schemes determine the sleep schedule for UEs as in the case without RN. With one awake subframe in a sleep cycle set aside for receiving data on the backhaul link, the sleep period of RN is then assigned to the common

DOI: 10.1002/dac

sleeping subframes of all UEs. Three revised LBPS schemes, namely *LteA-Aggr-U1*, *LteA-Split-U1*, and *LteA-Merge-U1*, are proposed to support the UE-first strategy in this paper.

On the other hand, a predefined threshold for power-saving performance of RN is given in the RN-first strategy. The threshold sets a demand on the number of RN's sleep subframes in a sleep cycle, which further affects the sleep pattern of all UEs. Therefore, the previously proposed LBPS schemes need to be revised in order to accommodate the new requirement imposed by the RN's threshold. Because the scheme of *LBPS-Aggr* compared with *LBPS-Split* and *LBPS-Merge* offers less flexibility in sleep scheduling, it cannot be adapted to support the RN-first strategy. Two revised schemes, namely *LteA-Split-R1* and *LteA-Merge-R1*, are proposed in this paper.

3.2. UE-first strategy

(1) *LteA-Aggr-U1*

As the simplest version of LBPS, *LteA-Aggr-U1* treats all UEs as a single group in determining the synchronous sleep schedule. The length of a sleep cycle in *LteA-Aggr-U1* is calculated according to the total downlink load of all UEs and the current estimation of the capacity in a subframe as follows:

$$\begin{aligned} &\textit{The length of the next sleep cycle } K \\ &= \textit{LengthAwkSlpCyl}(\lambda, \textit{Data\_TH}), \\ \text{where } \lambda &= \text{the total downlink load for all UEs, and} \\ \textit{Data\_TH} &= \text{the current estimation of the capacity for all UEs in a subframe.} \end{aligned}$$

The scheme of *LteA-Aggr-U1* is illustrated in Figure 4, in which two cases of the result in power saving are displayed. The typical case (Case A in Figure 4) is when the calculated cycle length K is larger than 2, meaning that there are K-2 subframes for RN power saving. Power saving efficiency for RN (defined as the ratio of the sleep period and denoted by PSE_{RN} in the

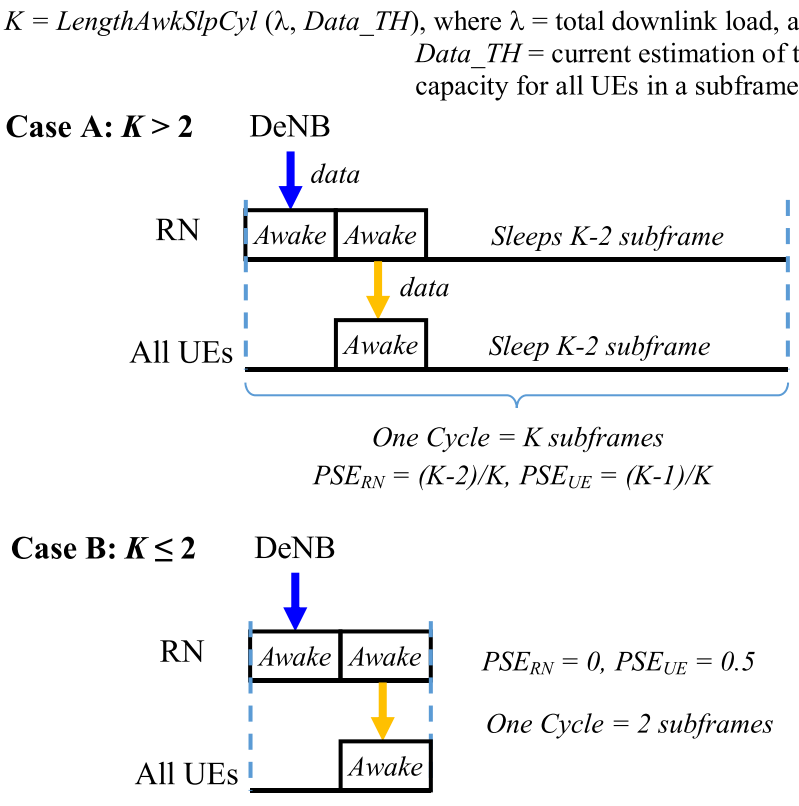

Figure 4. The scheme of *LteA-Aggr-U1*.

DOI: 10.1002/dac

figure) in the case is therefore *(K-2)/K*. On the other hand, the worst case for RN power saving (Case B in Figure 4) is when the calculated cycle length K is less than or equal to 2, resulting in zero power saving for RN and 50% power saving for UEs.

(2) *LteA-Split-U1*

Starting from a whole group of UEs as in *LteA-Aggr-U1*, *LteA-Split-U1* takes advantage of splitting operation to extend the sleep cycle length. The splitting operation is aimed at maximizing the cycle length of each split group for better power-saving efficiency. Figure 5 is used as an example for illustration of the typical *LteA-Split-U1* protocol. The first iteration of the example results in the cycle length of 3 (i.e., K_G =3), and a splitting operation is then performed in the second iteration. The cycle length of the second iteration (i.e., K =4 in the case) is the minimum value of K among the three split groups. The splitting operation stops when two consecutive iterations resulting in the same cycle length as iterations (3) and (4) in Figure 5. Iteration (4) is where the original version of *LBPS-Split* stops. In *LteA-Split-U1*, one subframe for the backhaul link is necessary for a feasible sleep schedule, which means the cycle length must be larger than the number of split groups at least by one. Iteration (4) fails

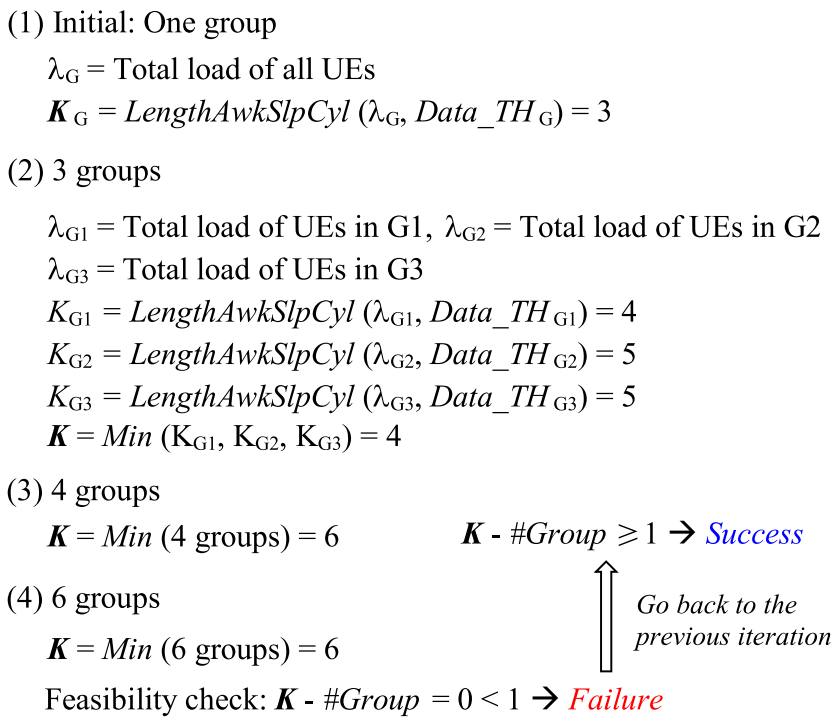

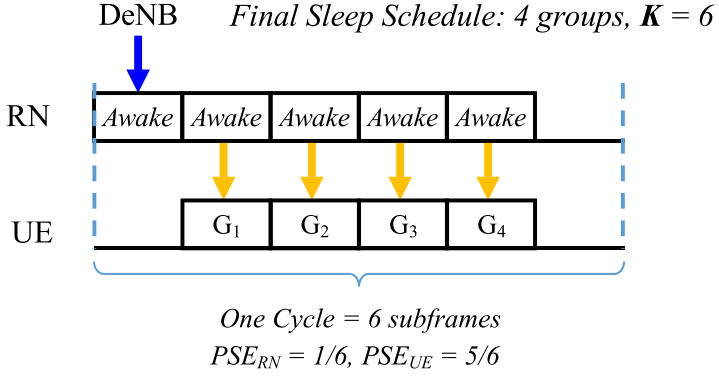

Figure 5. Example of *LteA-Split-U1*.

DOI: 10.1002/dac

to pass the feasibility check, and the result of the previous iteration, that is, four groups and the cycle length K =6 of iteration (3), is used for the final sleep schedule, as displayed in the lower part of Figure 5.

Note that the worst case of *LteA-Split-U1* in terms of power saving is when there is no space for splitting in the very beginning, which makes *LteA-Split-U1* behave the same as *LteA-Aggr-U1*.

(3) *LteA-Merge-U1*

Starting from each UE forming a single-member group, *LteA-Merge-U1* allows UEs to have a different cycle length in sleep schedule. As mentioned in Section 2-B, the cycle length calculated by the function of *LengthAwkSlpCyl* is converted to the closest and smaller power of 2 to simplify the check of schedulability. The major difference between *LteA-Merge-U1* and its original version of *LBPS-Merge* is the requirement of one subframe for the backhaul link in a sleep cycle, which also leads to the change of the equation of schedulability check. In the original version of *LBPS-Merge*, the equation of *Schedulability* is defined as follows:

$$Schedulability_{LBPS\text{-}Merge} = \sum_i \frac{1}{K_i^{\#}} \leqslant 1,$$

where $K_i^{\#}$ is the converted value of the cycle length of group i.

Considering the requirement of the subframe for the backhaul link, one more item is added to the equation of *schedulability* in *LteA-Merge-U1* as follows:

$$Schedulability_{LteA\text{-}Merge\text{-}U1} = \sum_i \frac{1}{K_i^{\#}} + \frac{1}{K_{Bkhl}} \leqslant 1,$$

where K_{Bkhl} is the cycle length for the backhaul link.

The value of K_{Bkhl} is set as the maximum cycle length among all groups in each iteration. An example of *LteA-Merge-U1* is given in Figure 6, in which there are 6 UEs under

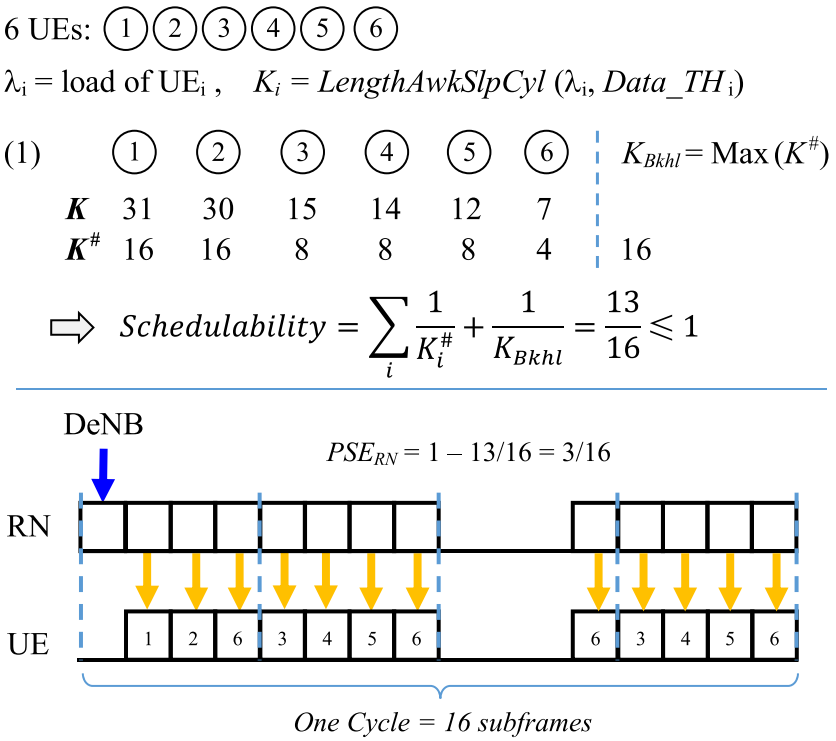

Figure 6. Example of *LteA-Merge-U1*: $PSE_{RN} > 0$.

DOI: 10.1002/dac

RN. The value of K in the figure is the original value of the cycle length calculated according to the load of each UE. The value of $K^{\#}$ is the converted value of K to the closest and smaller power of 2. Because the value of $Schedulability_{LteA\text{-}Merge\text{-}U1}$ in the first iteration is 13/16, which is less than 1, a feasible sleep schedule can be found with no need of merging operation. Moreover, the maximum value of $K^{\#}$ is 16; therefore, the cycle length of the sleep schedule is 16, and the awake subframe(s) for each UE can be determined according to the UE's $K^{\#}$. Power-saving efficiency for RN in this case is calculated as $PSE_{RN} = 1 - Schedulability_{LteA\text{-}Merge\text{-}U1} = 3/16$

It is easy to know from the example of Figure 6 that if $Schedulability_{LteA\text{-}Merge\text{-}U1} = 1$ in the final iteration in *LteA-Merge-U1*, there would be no space for RN power saving (i.e., $PSE_{RN} = 0$). To illustrate the case, Figure 7 shows a series of merge operation for another example of *LteA-Merge-U1* in order to find a feasible sleep schedule, resulting in zero power saving of RN. Because the value of $Schedulability_{LteA\text{-}Merge\text{-}U1}$ is larger than 1 in iteration (1) in Figure 7, merging some UEs is required. Two types of merge operation were defined in the authors' previous work [8], namely, the *non-degraded merge* and the *degraded merge*. A merge operation is defined as a degraded merge if merging two UEs resulted in a smaller $K^{\#}$ than both the original two values of $K^{\#}$. On the other hand, a non-degraded merge does not result in a smaller value of $K^{\#}$. For example, merging UE_1 and UE_2 in iteration (1) of Figure 7 is a degraded merge, because the new value of $K^{\#} = 8$ is smaller than the original values (i.e., 16). From the aspect of power saving, a non-degraded merge is preferred than a degraded merge, because a smaller value of $K^{\#}$ (in the case of a degraded merge) results in less power saving. Therefore, the scheme of *LteA-Merge-U1* searches all

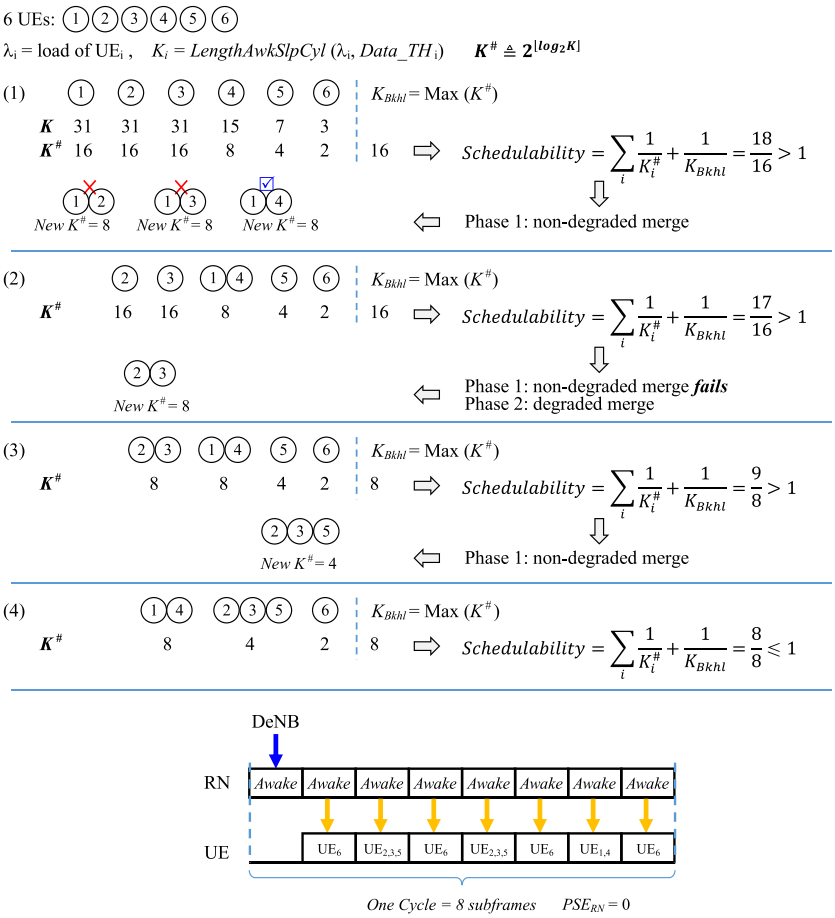

Figure 7. Example of *LteA-Merge-U1*: $PSE_{RN} = 0$.

DOI: 10.1002/dac

possible non-degraded merges before adopting a degraded merge as illustrated in iteration (1). The merging process ends when the value of $Schedulability_{LteA\text{-}Merge\text{-}U1}$ is less than or equal to 1 as displayed in iteration (4) of the example.

Note that the value of K_{Bkhl} changes during the merging process in Figure 7, because K_{Bkhl} is set as the maximum value of $K^{\#}$ among all groups in each iteration. Moreover, note that the worst case for *LteA-Merge-U1* in terms of power saving for both RN and UEs is when all UEs are finally merged into a whole group making the same result as *LteA-Aggr-U1*.

It is worth mentioning that in order to take advantage of *multi-user diversity* in resource allocation in a subframe, the constraint of minimum group size could be added in *LteA-Merge-U1* as well as in *LteA-Split-U1* to set a limitation for the merging/splitting process.

3.3. RN-first strategy

In the RN-first strategy, a threshold, namely RN_PSE_TH, is given as the goal for RN power saving. The value of RN_PSE_TH represents the ratio of time in which RN should be in the sleep mode. Therefore, RN_PSE_TH sets a limit of the cycle length in LBPS schemes. Because only *LBPS-Split* and *LBPS-Merge* can provide the flexibility of adjusting the sleep cycle length, two revised schemes, namely *LteA-Split-R1* and*LteA-Merge-R1*, are proposed under the RN-first strategy.

(1) *LteA-Split-R1*

As mentioned in the contrast scheme of *LteA-Split-U1* (under the UE-first strategy) in Section 3-B-(2), the final cycle length must accommodate one more subframe for the backhaul link in order to have a feasible sleep schedule. In *LteA-Split-R1*, the value of RN_PSE_TH sets another constraint for the final cycle length. Therefore, with the same splitting process, the only difference between *LteA-Split-R1* and *LteA-Split-U1* is the requirement in determining the final cycle length, given the value of the cycle length (K) and the number of split group (*#Group*) in an iteration. The requirements for *LteA-Split-U1* and *LteA-Split-R1* are given as follows.

LteA-Split-U1: $K - \#Group \geqslant 1$ (1 represents the need of one subframe for the backhaul link)

LteA-Split-R1: $\frac{K-\#Group-1}{K} \geqslant RN\_PSE\_TH$ (the ratio of RN sleep time must be larger than the threshold).

Note that if no proper value of the cycle length can be found to meet the requirement of RN_PSE_TH in *LteA-Split-R1*, the scheme goes back to the original state of *LteA-Aggr-U1* (all UEs in a group) and declares RN's power saving as zero.

(2) *LteA-Merge-R1*

A simple way to understand the impact of *RN_PSE_TH* on *LteA-Merge-R1* is by contrasting with the scheme of *LteA-Merge-U1*. The value of *RN_PSE_TH* represents the ratio of time in which RN should be in the sleep mode. More specifically, one subframe in the cycle of $K^{\#}_{RN\_PSE\_TH}$ subframes must be reserved for RN to enter the sleep mode, and the value of $K^{\#}_{RN\_PSE\_TH}$ in *LteA-Merge-R1* is calculated as follows.

$$K^{\#}_{RN\_PSE\_TH} = 2^{\lfloor log_2 K \rfloor}, \text{where } K = \frac{1}{\lfloor RN\_PSE\_TH \rfloor}$$

Because no link activity (on both the backhaul link and the access link) is allowed when RN is in the sleep mode, the equation of *Schedulability* in *LteA-Merge-R1* must include $K^{\#}_{RN\_PSE\_TH}$ as well. The new equation of *Schedulability* in *LteA-Merge-R1* is defined as follows.

$$Schedulability_{LteA\text{-}Merge\text{-}R1} = \sum_i \frac{1}{K^{\#}_i} + \frac{1}{K_{Bkhl}} + \frac{1}{K^{\#}_{RN\_PSE\_TH}} \leqslant 1,$$

$$\text{where } K_{Bkhl} = \text{Max}(K^{\#}_i, K^{\#}_{RN\_PSE\_TH})$$

DOI: 10.1002/dac

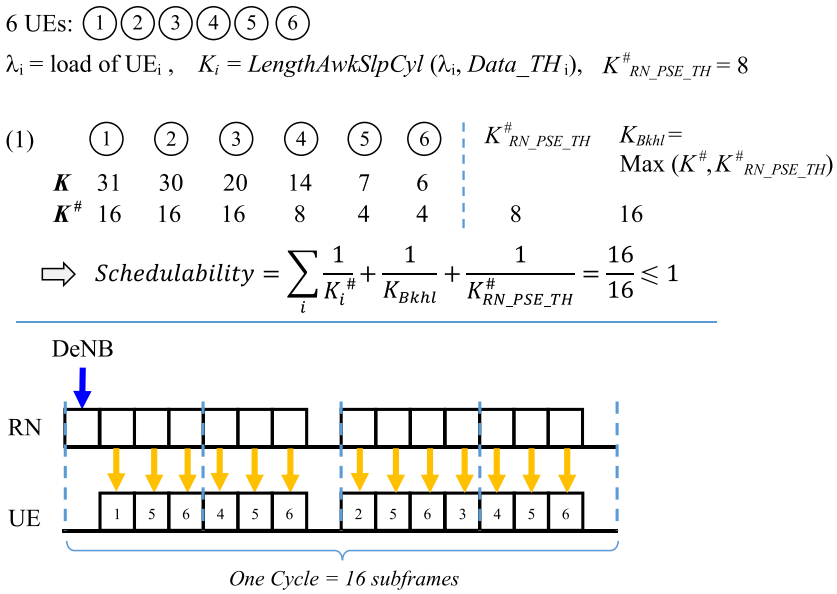

Figure 8. Example of *LteA-Merge-R1*: $RN\_PSE\_TH = 0.125$.

An example of *LteA-Merge-R1* is given in Figure 8 with $RN\_PSE\_TH = 0.125$, in which the value of $K^{\#}_{RN\_PSE\_TH}$ is 8 and the value of $Schedulability_{LteA\text{-}Merge\text{-}R1}$ is 16/16 in iteration (1), implying that a feasible sleep schedule can be found without further merge operation. Note that the worst case for *LteA-Merge-R1* is when the requirement of RN_PSE_TH cannot be met and the scheme goes back to the same result as in *LteA-Aggr-U1* and declares RN's power saving as zero.

4. PERFORMANCE EVALUATION

4.1. Simulation environment and metrics

A custom program developed by Microsoft Visual C++ for system level simulation is extended from the authors' previous tool in IEEE 802.16e. The simulated network consists of one DeNB, one RN, and 40 UEs. The input load for each UE is equal, and the packet arrival process for the downlink traffic is assumed to be Poisson. The size of a packet is 799 bits. The channel quality for each UE is simulated by directly drawing a random number from the range of CQI values. The number of bits that can be carried in a resource block is calculated according to the efficiency of the CQI value. Three types of UEs are defined for simulating different cases of the channel quality. An *H-type* (high link quality) UE is assumed to use 64QAM modulation with CQI value ranging from 10 to 15. An *M-type* (medium link quality) UE uses 16QAM with CQI ranging from 7 to 9. An *L-type* (low link quality) UE uses QPSK with CQI ranging from 1 to 6. In addition to the proposed schemes, a contrast scheme based on standard DRX (denoted by *Std. DRX*) is also simulated. Parameters used in the simulation are summarized in Table I.

Four performance metrics are investigated in the simulation study as defined in the following:

(1) *Power-saving efficiency*, denoted by *PSE*, is defined as the ratio of time in the sleep mode. *PSE* for UEs and RN is calculated independently in the simulation.
(2) *Average delay*, denoted by *AvgDelay*, is defined as the average access delay for all downlink packets.
(3) *DRX signaling overhead*, denoted by *SignalDRX*, is defined as the average number of DRX control message per radio frame (10 ms) per UE. In LBPS schemes, to start a new sleep cycle for a UE, a DRX reconfiguration message is sent out by RN to the UE notifying of the new cycle length. Therefore, the value of *SignalDRX* is affected by the length of the sleep cycle.

DOI: 10.1002/dac

Table I. Simulation parameters.

Channel capacity	20 MHz (#RB = 100)
#DeNB, #RN, # UE	1, 1, 40 (UE with equal load)
Type of UE	*H-type*: CQI 11∼15 *M-type*: CQI 6∼ 10 *L-type*: CQI 1∼ 5
Packet size	799 bits
DATA_TH	Estimated capacity × 0.8
Prob_TH	0.8
Minimum group size	2
Contrast scheme *Std. DRX*	On duration = 1ms Inactivity timer = 10ms Short DRX cycle = 80ms Short cycle timer = 2 Long DRX cycle = 320ms

Table II. Summary of all schemes in the simulation study.

Strategy	Scheme name	Remark
UE-first (U1)	*LteA-Aggr-U1* *LteA-Split-U1* *LteA-Merge-U1*	PSE results include *UE's PSE* and *RN's PSE*.
	Std. DRX	The contrast scheme
RN-first (R1)	*LteA-Split-R1* *LteA-Merge-R1*	PSE results include *UE's PSE* and *RN's PSE*.

(4) *CQI report signaling overhead*, denoted by *SignalCQI*, is defined as the number of CQI report message per radio frame per UE. The default CQI report period is set as 5 ms (i.e., two CQI reports in a radio frame), which is subject to change because of the DRX operation.

Because many schemes are involved in the simulation study, a summary of all simulated schemes is given in Table II for better understanding the simulation results in the following sections. Note that because the proposed schemes under the UE-first strategy and the RN-first strategy support integrated power saving for RN and UEs, there are two curves of *PSE*, one for RN and the other for UEs, for an individual scheme. The contrast scheme of *Std. DRX* cannot support power saving for RN; therefore, it is not simulated under the RN-first strategy.

4.2. Results of UE-first strategy

The results of *PSE* for different UE cases are displayed in Figures 9–11, and the corresponding results of *AvgDelay* are displayed in Figures 12–14. Note that the result of RN's *PSE* for *Std. DRX* is zero in all UE cases, which is not displayed in Figures 9–11. The following observations can be made from these figures.

(1) *LteA-Split-U1* and *LteA-Merge-U1* outperform *LteA-Aggr-U1* and Std. DRX in terms of UE's PSE as well as RN's PSE at the cost of slightly increased *AvgDelay*, which demonstrates the benefit of grouping UEs (either by splitting or merging) in sleep scheduling.
(2) As displayed in Figures 9 and 10, *LteA-Split-U1* outperforms *LteA-Merge-U1* in most cases in terms of UE's PSE and RN's PSE, because the conversion of the cycle length (to a power of 2) in *LteA-Merge-U1* results in lower PSE for both UE and RN. There are a few cases, that is, λ =33.7Mbps and 39.3Mbps in Figure 9 and λ =17.1Mbps in Figure 10, that *LteA-Merge-U1* is better than *LteA-Split-U1* in terms of UE's PSE. The reason is the flexibility of allowing multiple sleep cycle lengths in *LteA-Merge-U1* provides more benefit in UE's PSE

DOI: 10.1002/dac

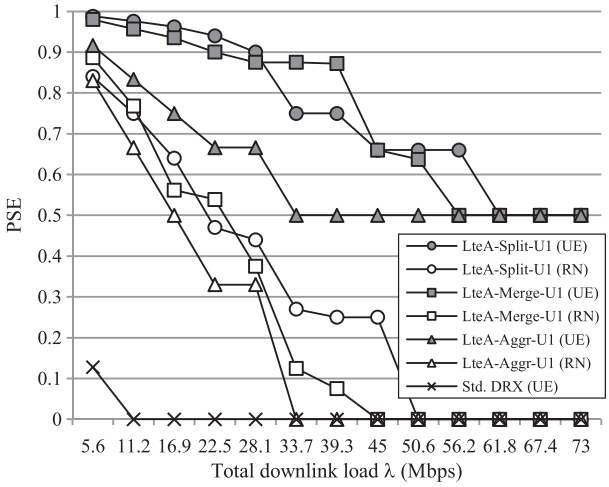

Figure 9. *PSE* of U1 strategy: All-H user equipments.

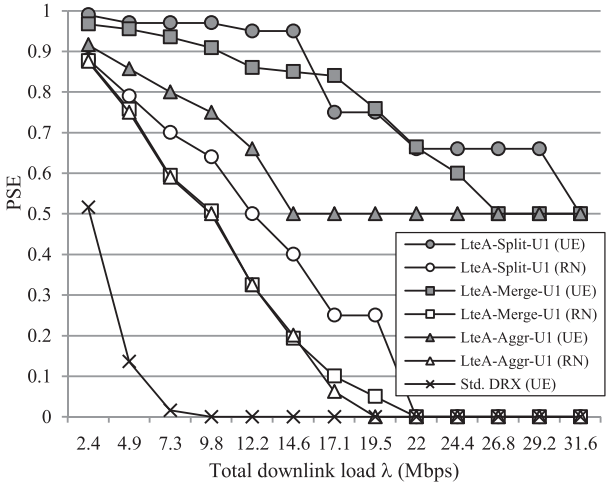

Figure 10. *PSE* of U1 strategy: All-M user equipments.

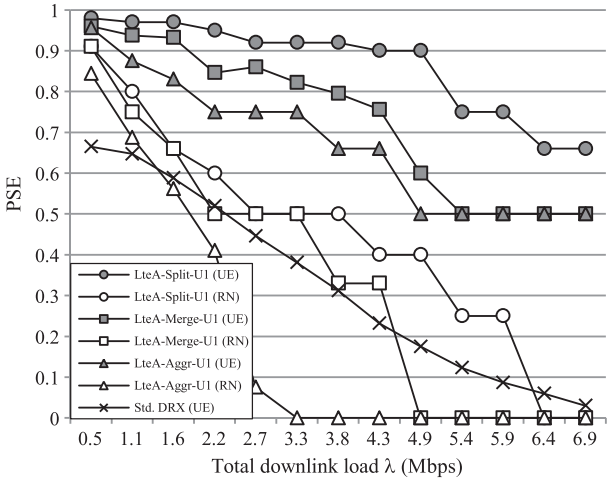

Figure 11. *PSE* of U1 Strategy: All-L user equipments.

DOI: 10.1002/dac

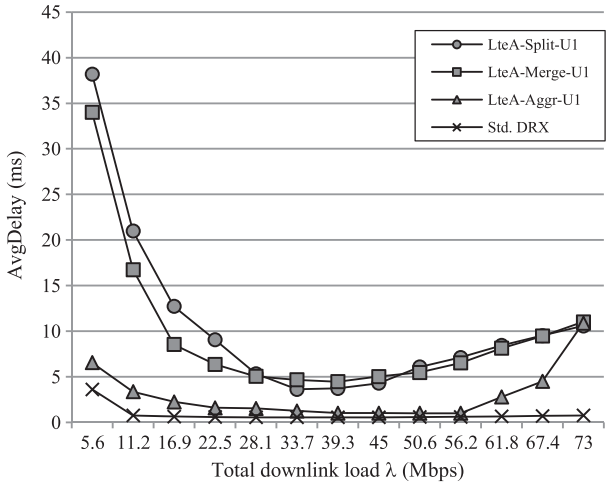

Figure 12. *AvgDelay* of U1 Strategy: All-H user equipments.

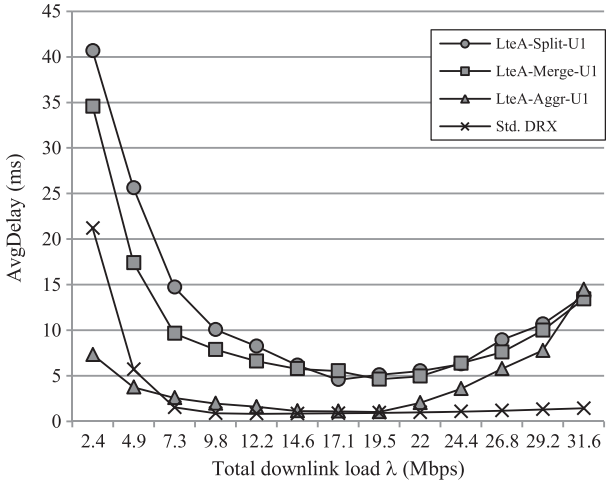

Figure 13. *AvgDelay* of U1 strategy: All-M user equipments.

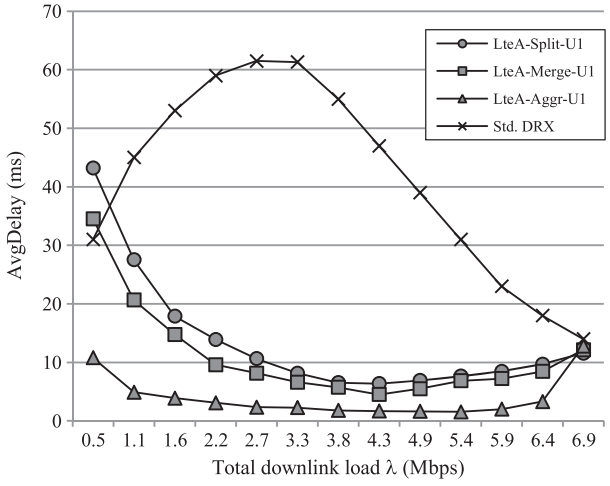

Figure 14. *AvgDelay* of U1 strategy: All-L user equipments.

DOI: 10.1002/dac

and therefore compensates the loss of UE's PSE due to the conversion of the cycle length to a power of 2.

(3) RN's PSE for *Std. DRX* is zero even in very light load, because for 40 UEs, the probability of all UEs entering the sleep period at the same time is very close to zero, making RN never obtain the chance of power saving in the simulation.

(4) As shown in Figure 11, UE's PSE of *Std. DRX* is better than the proposed schemes for some input loads in the case of All-L UEs, because the packet arrival rate with fixed size (799 bits) is very low, triggering the inactivity timer of *Std. DRX* to expire more frequently and achieve higher UE's PSE at the cost of high *AvgDelay* as shown in Figure 14.

(5) The behavior of *AvgDelay* with the increase of the input load for all schemes in Figure 12–14 is different from what we usually expect according to the queuing theory. The reason is the network system with power saving is non-work-conserving, and the average delay is affected not only by the input load but also the power-saving mechanism. More specifically, both the increase of load and the increase of PSE contribute to the increase of *AvgDelay*. However, load increasing makes lower PSE. Therefore, as the load increases, the curve of *AvgDelay* will either go up or go down, depending on which factor makes a higher impact on the average delay. For the proposed schemes of *LteA-Aggr-U1*, *LteA-Split-U1*, and *LteA-Merge-U1*, considering the range of load from light to medium (e.g., λ =5.6–33.7 Mbps in Figure 12 and λ =2.4–14.6 Mbps in Figure 13), the impact of increasing load on *AvgDelay* is less than the

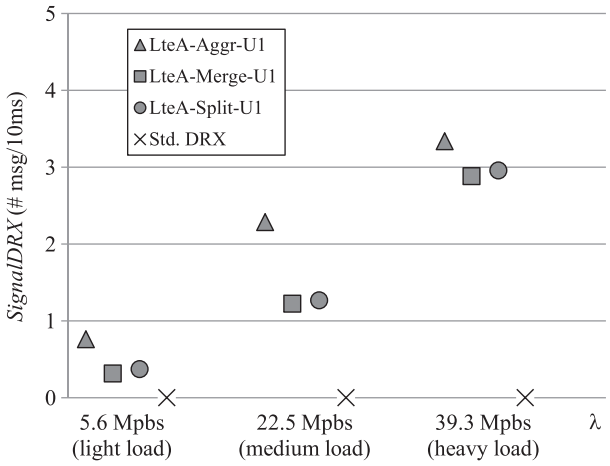

Figure 15. *SignalDRX* of U1 strategy: All-H user equipments.

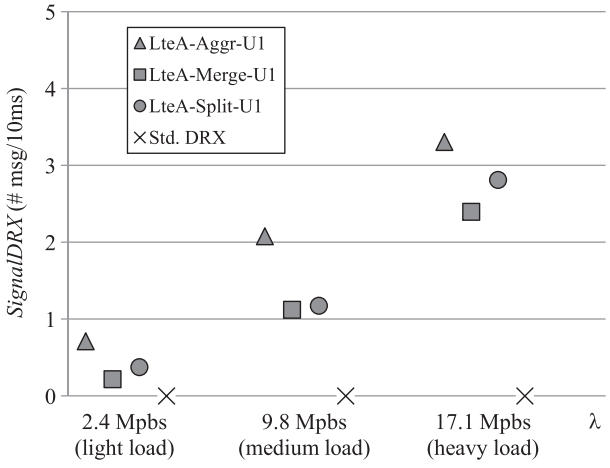

Figure 16. *SignalDRX* of U1 strategy: All-M user equipments.

DOI: 10.1002/dac

impact of decreasing PSE. Therefore, the curves of *AvgDelay* have a decreasing tendency. On the other side of the load from medium to heavy, the curves of *AvgDelay* go up as the load increases because of the fact that PSE in the case has little impact on *AvgDelay* because it is almost reaching the boundary condition.

Results of *SignalDRX* and *SignalCQI* under three different data rates are displayed in Figures 15–17 and Figures 18–20. The following observations can be made from the figures.

(1) *SignalDRX* of *LteA-Aggr-U1* is larger than that of *LteA-Split-U1* and *LteA-Merge-U1* in all cases because the smaller sleep cycle length by *LteA-Aggr-U1* results in more frequent notification of the next cycle length. The same reason is also applied to higher *SignalCQI* of *LteA-Aggr-U1* than that of *LteA-Split-U1* and *LteA-Merge-U1* in CQI reporting. Moreover, as the input load increases, *SignalDRX* and *SignalCQI* of the three LBPS schemes increase because of the decreased sleep cycle length.
(2) Because DRX configuration for *Std. DRX* is fixed after initialization, *SignalDRX* values of the *Std. DRX* scheme is zero. On the other hand, the value of *SignalCQI* for *Std. DRX* increases as the load increases, because under heavier load, the chance for the *Std. DRX* scheme entering the DRX mode is becoming lower, which results in more CQI reporting for packet scheduling.

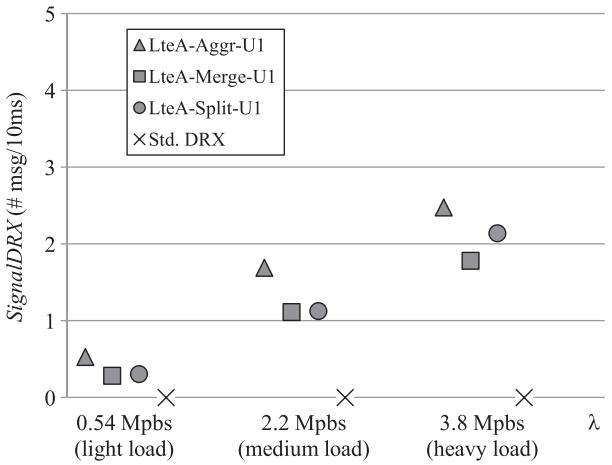

Figure 17. *SignalDRX* of U1 strategy: All-L user equipments.

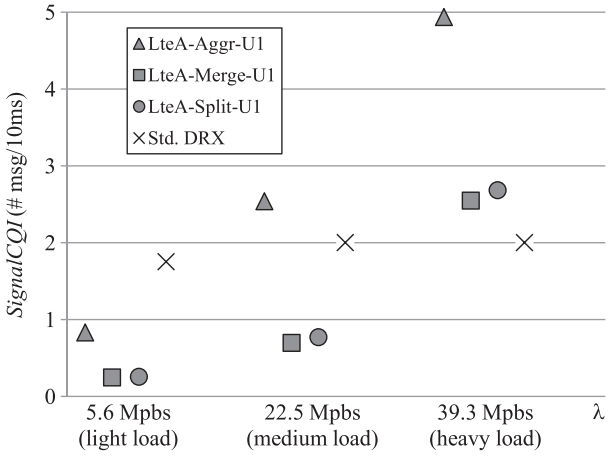

Figure 18. *SignalCQI* of U1 strategy: All-H user equipments.

DOI: 10.1002/dac

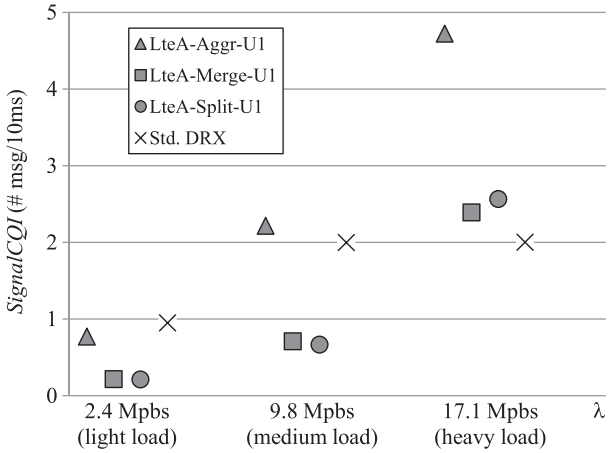

Figure 19. *SignalCQI* of U1 strategy: All-M user equipments.

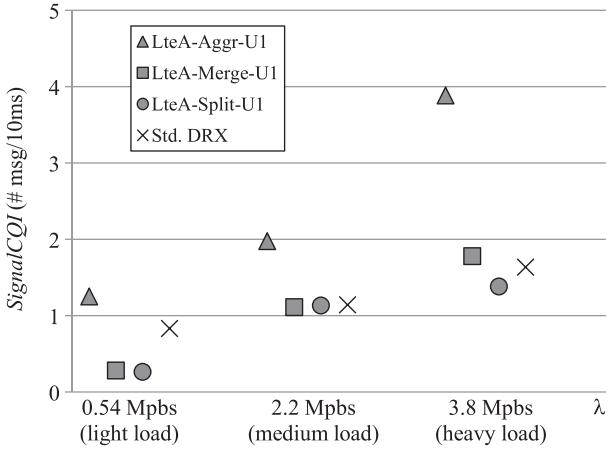

Figure 20. *SignalCQI* of U1 strategy: All-L user equipments.

4.3. Results of RN-first Strategy

PSE and *AvgDelay* of the RN-first Schemes (*LteA-Split-R1*, *LteA-Merge-R1*) with $RN\_PSE\_TH = 0.125$ for the case of *All-M UEs* are displayed in Figures 21 and 22, respectively. As we can see in Figure 21, the goal of RN_PSE_TH can be achieved by both schemes when the input load is not too heavy (e.g., under 14.6 Mbps in the figure). As the input load becomes heavier (e.g. 22 Mpbs or higher in the figure), both RN-first schemes can no longer meet the goal of RN_PSE_TH because both schemes fails to accommodate RN_PSE_TH in sleep scheduling. Figure 21 also shows that better *RN's PSE* is achieved by *LteA-Split-R1* than *LteA-Merge-R1* at the cost of slightly decreased *UE's PSE*. On the other hand, the relationship of*UE's PSE* of the two schemes in Figure 21 is reflected in the relationship of *AvgDelay* in Figure 22.

The *PSE* results for the two RN-first schemes under different values of RN_PSE_TH (1/4, 1/8, 1/16) are displayed in Figures 23 and 24, showing that a higher RN_PSE_TH makes lower UE's *PSE* in both schemes.

4.4. Comparison of the two strategies

By comparing UE's *PSE* and RN's *PSE* in Figure 10 (UE-first) with those in Figures 23 and 24 (RN-first), it is found that the UE-first schemes (*LteA-Split-U1* vs. *LteA-Split-R1*, *LteA-Merge-U1* vs. *LteA-Merge-R1*) outperform the corresponding RN-first schemes not only in terms of UE's *PSE* but also in terms of RN's *PSE*. In the case of light load, it is reasonable for UE-first schemes to

DOI: 10.1002/dac

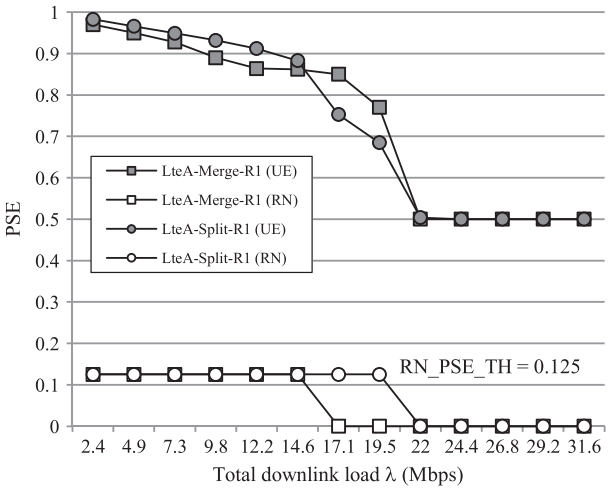

Figure 21. *PSE* of R1 strategy: All-M user equipments.

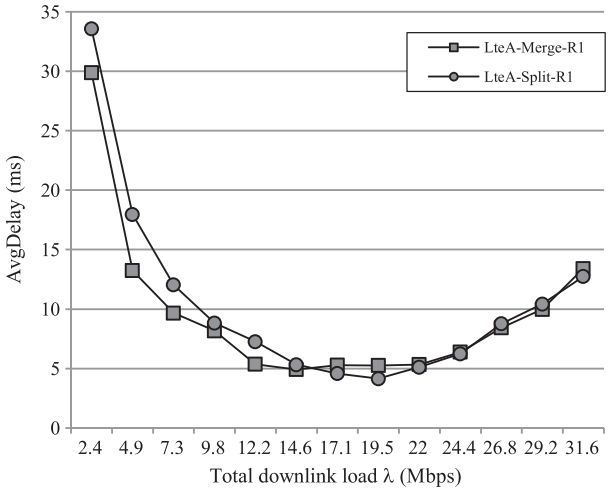

Figure 22. *AvgDelay* of R1 strategy: All-M user equipments.

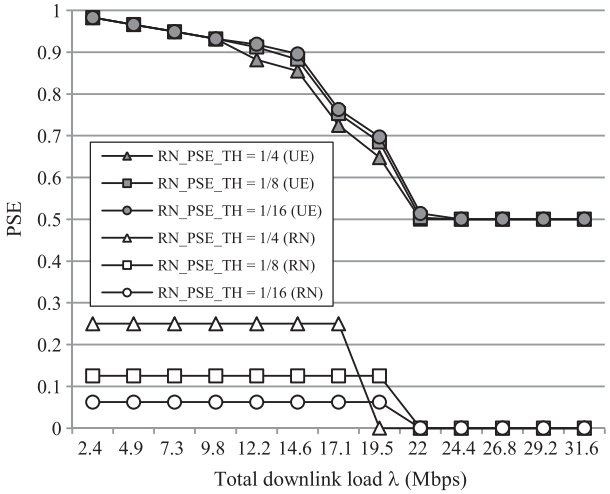

Figure 23. *PSE* of *LteA-Split-R1*: All-M user equipments.

DOI: 10.1002/dac

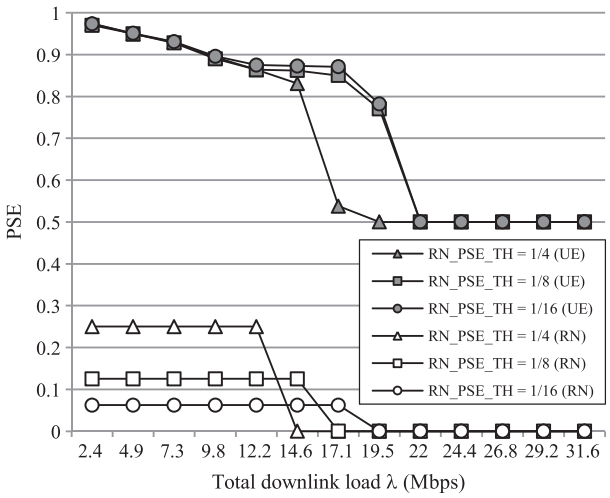

Figure 24. *PSE* of *LteA-Merge-R1*: All-M user equipments.

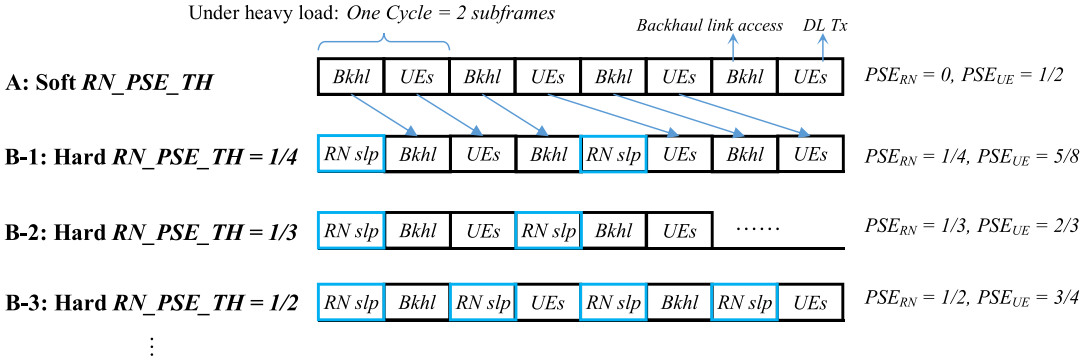

Figure 25. Examples of *Hard* RN_PSE_TH.

achieve higher RN's *PSE* because there is more space for RN sleeping than the given values of RN_PSE_TH. In the case of heavy load, the proposed two RN-first schemes fail to meet the requirement of RN_PSE_TH because of the design philosophy of the schemes as explained in the following.

Although named as RN-first schemes, *LteA-Split-R1* and *LteA-Merge-R1* are intrinsically load-based, which means the input load of UEs plays the key role in integrated sleep scheduling. The idea of LBPS makes the RN-first schemes in a sense of '*soft*' RN_PSE_TH instead of '*hard*' RN_PSE_TH. The comparison between *soft* RN_PSE_TH and *hard* RN_PSE_TH under the heavy load is illustrated in Figure 25, in which the example under *soft* RN_PSE_TH (part A in the figure) treats UE's scheduling as the major concern, while the examples under *hard* RN_PSE_TH (part B-1– B-3 in the figure) make RN's power saving as the first priority. As shown in Figure 25, a higher *hard* RN_PSE_TH makes UE's *PSE* even higher in the heavy load, which is actually not preferred from the aspect of access delay.

In summary, we conclude that the UE-first schemes are more preferred than the RN-first schemes for integrated sleep scheduling of UEs and RN.

4.5. Further discussion

In this section we would like to compare the performance of the two grouping mechanisms, *splitting* and *merging*, for integrated sleep scheduling. So far, the *PSE* results we have shown is all in the case of the equal load. It is observed that under the equal load, the schemes adopting the splitting mechanism (*LteA-Split-U1* and *LteA-Split-R1*) outperform the schemes adopting the merging mechanism

DOI: 10.1002/dac

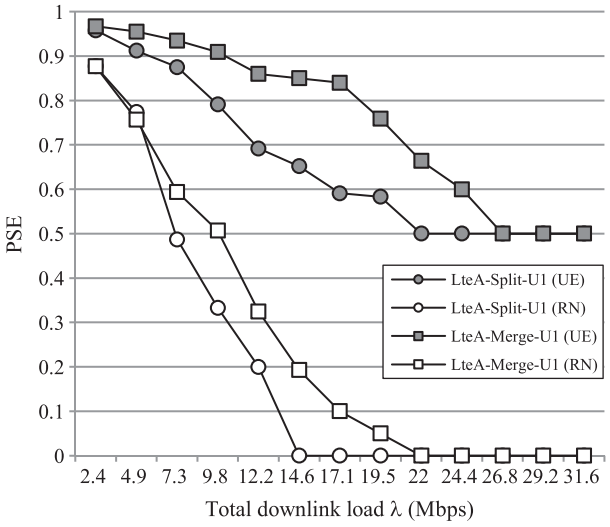

Figure 26. *LteA-Split-U1* vs. *LteA-Merge-U1* (8:2 load).

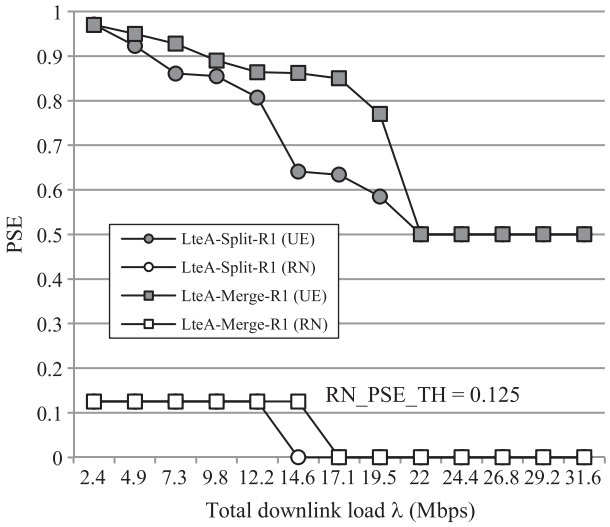

Figure 27. *LteA-Split-R1* vs. *LteA-Merge-R1* (8:2 load).

(*LteA-Merge-U1* and *LteA-Merge-R1*) in terms of UE's and RN's PSE. However, the said observation no longer holds when the input load distribution among UEs is not equal. Figure 26 and 27 show the *PSE* results of the two grouping mechanisms under '*8:2 load*', in which 80% of the traffic load goes to 20% of the UEs. The figures demonstrate the benefit of the merging mechanism in the case of higher variation in traffic load distribution, because the merging mechanism allows different sleep cycle length for different groups of UEs.

Lastly, although it is not a typical scenario, the impact of a *worse backhaul link* on *PSE* is also investigated. The scenario is simulated by assigning *M-type* CQIs (6–10) to the backhaul link and *H-type* CQIs (11–15) to the access links. Because the estimation of the sleep cycle length in the proposed schemes is according to the input load of the UEs, the worse backhaul link does not make different *PSE* results. However, the access delay is increased because of the congested state on the backhaul link. In order to cope with the situation of a worse backhaul link, the calculation of the sleep cycle length should be revised to be based on the actual traffic load that can be transmitted on the backhaul link instead of the original arrival rate from the Internet. By taking *LteA-Split-U1* as an example, Figure 28 shows the*PSE* results of the old calculation (denoted by *LteA-Split-U1-OLD*)

DOI: 10.1002/dac

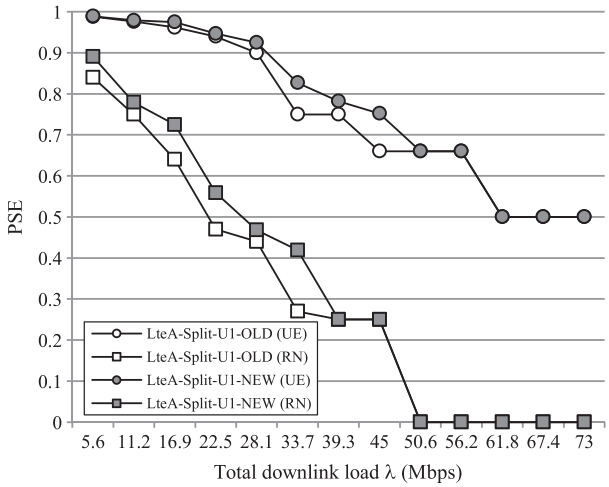

Figure 28. *PSE* of *LteA-Split-U*1 under a worse backhaul link.

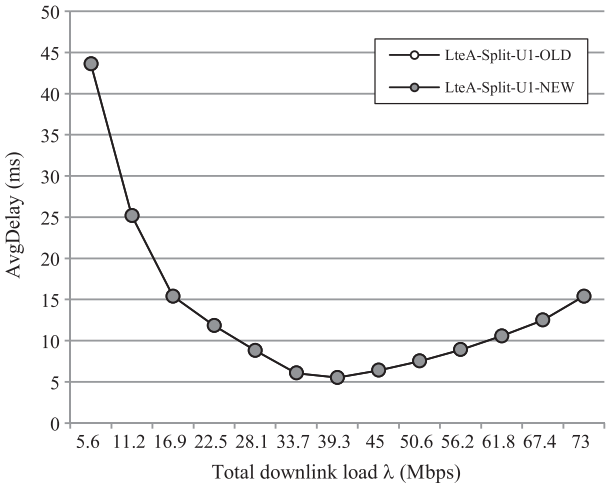

Figure 29. *AvgDelay* of *LteA-Split-U1* under a worse backhaul link.

and the revised calculation (denoted by *LteA-Split-U1-NEW*). The corresponding result of *AvgDelay* is displayed in Figure 29. The figures show that higher *PSE* can be achieved by the revised calculation of the sleep cycle length without increasing *AvgDelay*.

5. CONCLUSION

In this paper, the authors focus on integrated power saving for both RN and UEs in LTE-A. Based on the authors' previously proposed idea of LBPS, two integration strategies, namely, UE-first and RN-first, each with a couple of associated schemes, are proposed. Simulation study shows that by taking advantage of grouping UEs either by splitting or merging in sleep scheduling, higher power saving efficiency can be achieved at the cost of moderate increase in the average access delay. It is also concluded that under the idea of soft threshold for RN's power saving, the proposed schemes under the UE-first strategy are preferred than their counterparts under the RN-first strategy. Further investigations on performance comparison of the splitting and the merging mechanisms are also presented. Because the benefit of the merging mechanism over the splitting mechanism in terms of power-saving efficiency lies in the flexibility of different cycle length in sleep scheduling, the merging mechanism outperforms the splitting mechanism in the case of various load among UEs.

DOI: 10.1002/dac

Lastly, the scenario of a worse backhaul link (in comparing with the access link) is also investigated. Revised calculation for the sleep cycle length is proposed to increase power-saving efficiency without increasing the access delay.

ACKNOWLEDGEMENTS

This work was supported in part by the Ministry of Science and Technology, Taiwan, R.O.C., under grant no. MOST 103-2221-E-260-021.

REFERENCES

1. 3GPP TS 36.300. Evolved universal terrestrial radio access (E-UTRA) and evolved universal terrestrial radio access network (E-UTRAN), Rel. 8, v8.5.0, May 2008.
2. 3GPP TR 36.806. Evolved universal terrestrial radio access (E-UTRA) relay architectures for E-UTRA (LTE-Advanced), Rel. 9, v9.0.0, Mar. 2010.
3. 3GPP TS 36.300. Evolved universal terrestrial radio access (E-UTRA) and evolved universal terrestrial radio access network (E-UTRAN), Rel. 10, v10.3.0, Mar. 2011.
4. 3GPP TR 36.836. Evolved universal terrestrial radio access (E-UTRA): study on mobile relay, Rel. 12, v12.0.0, Jun 2014.
5. Yu YP, Feng KT. Traffic-based DRX cycles adjustment scheme for 3GPP LTE systems. *Proceedings, IEEE Vehicular Technology Conference (VTC Spring)*, Yokohama, Japan, 2012; 1–5.
6. Jha SC, Koc AT, Vannithamby R. Optimization of discontinuous reception (DRX) for mobile internet applications over LTE. *Proceedings, IEEE Vehicular Technology Conference (VTC Fall)*, Quebec City, Canada, 2012; 1–5.
7. Jha SC, Koc AT, Vannithamby R, Torlak M. Adaptive DRX configuration to optimize device power saving and latency of mobile applications over LTE advanced network. *Proceedings, IEEE International Conference on Communications (ICC)*, Budapest, Hungary, 2013; 6210–6214.
8. Yang CC, Mai YT, Chen JY, Shen YS, Kuo YC. LBPS: load-based power saving in the IEEE 802.16e network. *Computers and Electrical Engineering* 2012; **38**(4):891–905.
9. Yang CC, Mai YT, Chen JY, Kuo YC. Integrated load-based power saving for BS and MSS in the IEEE 802.16e network. *Wireless Communications and Mobile Computing* 2015; **15**(4):601–614.
10. Yang CC, Chen JY, Mai YT, Liang CH. Design of a load-based DRX scheme for non-real-time traffic in LTE. *Proceedings, IAENG International Conference on Communication Systems and Applications (International Multiconference of Engineers and Computer Scientists, IMECS)*, Vol. II, Hong Kong, China, 2014; 657–662.
11. Ma Z, Zhang Y, Zheng K, Wang W, Wu M. Performance of 3GPP LTE-advanced networks with type i relay nodes. *Proceedings, International ICST Conference on Communications and Networking in China (CHINACOM)*, Beijing, China, 2010; 1–5.
12. Krishnan N, Panchal JS, Mandayam NB, Roy YD. Bandwidth sharing in LTE-A relaying systems. *Proceedings, Allerton Conference on Communication, Control, and Computing (Allerton)*, Allerton, IL, USA, 2010; 1125–1128.
13. Roth S, Gan J, Danev D. Subframe allocation for relay networks in the LTE advanced standard. *Proceedings, International Symposium on Personal Indoor and Mobile Radio Communications (PIMRC)*, Instanbul, Turkey, 2010; 1758–1763.
14. Zhao Z, Wang J, Redana S, Raaf B. Downlink resource allocation for LTE-Advanced networks with type1 relay nodes. *Proceedings, IEEE Vehicular Technology Conference (VTC Fall)*, Quebec City, Canada, 2012; 551–556.
15. Yi S, Lei M. Backhaul resource allocation in LTE-Advanced relaying systems. *Proceedings, IEEE Wireless Communications and Networking Conference (WCNC)*, Shanghai, China, 2012; 1207–1211.
16. Kifle DW, Bulakci O, Saleh AB, Redana S, Granelli F. Joint backhaul co-scheduling and relay cell extension in LTE-Advanced networks uplink performance evaluation. *Proceedings, European Wireless Conference (EW)*, Poznan, Poland, 2012; 1–8.
17. Song SH, Almutairi AF, Letaief KB. Outage-capacity based adaptive relaying in LTE-Advanced networks. *Proceedings, IEEE Transactions on Wireless Communications* 2013; **12**(9):4778–4787.
18. Vitiello F, Riihonen T, Hämäläinen J, Redana S. On buffering at the relay node in LTE-Advanced. *Proceedings, IEEE Vehicular Technology Conference (VTC Fall)*, San Francisco, CA, USA, 2011; 1–5.
19. Lin PC, Cheng RG, Chang YJ. A dynamic flow control algorithm for LTE-Advanced relay networks. *Proceedings, IEEE Transactions on Vehicular Technology* 2014; **63**(1):334–343.
20. Samdanis K, Brunner M. Self-organized network management functions for relay enhanced LTE-Advanced systems. *Proceedings, International Symposium on Personal Indoor and Mobile Radio Communications (PIMRC)*, Toronto, ON, Canada, 2011; 227–231.
21. Alam MS, Mark JW, Shen X. Relay selection and resource allocation for multi-user cooperative LTE-A uplink. *Proceedings, IEEE International Conference on Communications (ICC)*, Ottawa, ON, Canada, Jun 2012; 5092–5096.
22. Yun S, Park K, Lee S, Choi JK. Energy efficient relay selection scheme with DRX mechanism in 3GPP LTE network. *Proceedings, International Conference on ICT Convergence (ICTC)*, Jeju, Korea, 2013; 6–11.
23. Teyeb O, Frederiksen F, Phan VV, Raaf B. User multiplexing in relay enhanced LTE-advanced networks. *Proceedings, IEEE Vehicular Technology Conference (VTC Spring)*, Taipei, Taiwan, 2010; 1–5.

DOI: 10.1002/dac

24. Krendzel A. LTE-A mobile relay handling: architecture aspects. *Proceedings, 19th European Wireless Conference (EW)*, Guildford, UK, 2013; 1–6.
25. Tu H, Lin J, Chang T, Feng K. Prediction-based handover schemes for relay-enhanced LTE-A systems. *Proceedings, IEEE Wireless Communications and Networking Conference (WCNC)*, Shanghai, China, 2012; 2879–2884.

DOI: 10.1002/dac